

BER Performance of Joint THP/pre-FDE

Kazuki TAKEDA⁺ Hiromichi TOMEBA⁺ and Fumiyuki ADACHI[‡]

Dept. of Electrical and Communications Engineering, Graduate School of Engineering, Tohoku University
6-6-05 Aza-Aoba, Aramaki, Aoba-ku, Sendai, 980-8579 JAPAN

⁺{kazuki, tomeba}@mobile.ecei.tohoku.ac.jp [‡]adachi@ecei.tohoku.ac.jp

Abstract—Recently, frequency-domain equalization (FDE) based on the minimum mean square error (MMSE) criterion has been attracting much attention to overcome the frequency-selective fading channel. The bit error rate (BER) performance of single-carrier (SC) transmission is significantly improved by using MMSE-FDE by obtaining the frequency-diversity gain while suppressing the inter-symbol interference (ISI). However, the residual ISI after MMSE-FDE limits the performance improvement. Recently, we have proposed a joint use of Tomlinson-Harashima precoding (THP) and FDE reception (joint THP/FDE) to suppress the residual ISI. However, joint THP/FDE requires the channel state information (CSI) at both the transmitter and receiver. In this paper, we replace FDE reception by pre-FDE and propose joint THP/pre-FDE that requires the CSI at the transmitter only, while providing almost the same BER performance as joint THP/FDE.

Keywords—components; Single-carrier, pre-equalization, THP

I. INTRODUCTION

For the next generation mobile communication systems, high-speed and high-quality packet data services are demanded. Since the broadband wireless channel is composed of many propagation paths having different time delays, the bit error rate (BER) performance of single-carrier (SC) transmission significantly degrades due to inter-symbol interference (ISI) arising from frequency-selective fading channel [1]. The use of frequency-domain equalization (FDE) based on the minimum mean square error (MMSE) criterion improves the BER performance [2-5]. However, the residual ISI which remains after FDE limits the performance improvement [4].

Recently, Tomlinson-Harashima precoding (THP) [6, 7] has been attracting much attention as an effective technique to suppress the interference [8, 9]. In Refs. [10, 11], we have proposed a joint use of THP and FDE reception (in this paper, we call this equalization technique a joint THP/FDE) for SC transmission. THP is introduced to suppress the residual ISI. Joint THP/FDE requires the channel state information (CSI) at both the transmitter and the receiver. With the perfect CSI, the residual ISI can be completely removed. If FDE reception is replaced by pre-equalization, the mobile receiver structure for downlink (base-to-mobile) transmission can be simplified. For uplink (mobile-to-base) transmission, joint use of FDE reception and the ISI canceling technique [12, 13] can be used at the base station to simply the mobile transmitter. In this paper, we consider the downlink transmission. So far, some pre-equalization techniques have been proposed [14-16]. It was shown [16] that, with the perfect CSI, pre-FDE can provide almost the same BER performance as FDE reception.

In this paper, we replace FDE reception by pre-FDE and propose joint THP/pre-FDE that requires the CSI at the transmitter only, while providing almost the same BER performance as joint THP/FDE.

The remainder of this paper is organized as follows. Joint THP/FDE is described in Sec. II. Then, Sec. III presents joint THP/pre-FDE. In Sec. IV, the BER performance is evaluated by computer simulation. Sec. V concludes this paper.

II. JOINT THP/FDE

In this paper, symbol-time discrete signal representation is used. The channel is assumed to be an L -path frequency-selective block fading channel. The channel impulse response is given by

$$h(\tau) = \sum_{l=0}^{L-1} h_l \delta(\tau - \tau_l), \quad (1)$$

where h_l and τ_l respectively denote the path gain and the time delay of the l th path. We assume $\sum_{l=0}^{L-1} E[|h_l|^2] = 1$.

At the transmitter, N_g -symbol guard interval (GI) is inserted into the front of N_c -data symbol and (N_c+N_g) -symbol block is transmitted. With representing the N_c -data symbol block as a vector $\mathbf{s}=[s(0), \dots, s(N_c-1)]^T$, the received signal block after the removal of GI can be expressed using the vector form as

$$\mathbf{r} = [r(0), \dots, r(N_c-1)]^T = \sqrt{\frac{2E_s}{T_s}} \mathbf{h} \mathbf{s} + \mathbf{n}, \quad (2)$$

where E_s and T_s represent the average symbol energy and the symbol duration, respectively. $\mathbf{n}=[n(0), \dots, n(N_c-1)]^T$ represents the additive white Gaussian noise (AWGN) vector, whose elements are the zero-mean AWGN processes. The variance of each elements of \mathbf{n} is $2N_0/T_s$. N_0 is the one-sided noise power spectrum density. \mathbf{h} is an $(N_c \times N_c)$ channel matrix given by

$$\mathbf{h} = \begin{bmatrix} h_0 & & & & h_{L-1} & \cdots & h_1 \\ h_1 & h_0 & & & & \ddots & \vdots \\ \vdots & h_1 & h_0 & & \mathbf{0} & & h_{L-1} \\ h_{L-1} & \vdots & h_1 & \ddots & & & \\ & h_{L-1} & \vdots & \ddots & h_0 & & \\ & & h_{L-1} & & h_1 & h_0 & \\ \mathbf{0} & & & \ddots & \vdots & h_1 & h_0 \end{bmatrix}. \quad (3)$$

At the receiver, N_c -point fast Fourier transform (FFT) is applied to the received signal vector \mathbf{r} to transform into the frequency-domain signal. The frequency-domain signal is multiplied by the FDE weight and is transformed back to the time-domain signal by applying N_c -point inverse FFT (IFFT). The received signal vector after FDE is given by

$$\begin{aligned}\hat{\mathbf{r}} &= [\hat{r}(0), \dots, \hat{r}(N_c - 1)]^T \\ &= \sqrt{\frac{2E_s}{T_s}} \hat{\mathbf{h}} \mathbf{s} + \hat{\mathbf{n}}\end{aligned}\quad (4)$$

where $\hat{\mathbf{h}}$ is an $N_c \times N_c$ composite channel matrix of the propagation channel plus FDE, which is called equivalent channel matrix here, given by

$$\hat{\mathbf{h}} = \begin{bmatrix} \hat{h}_0 & \hat{h}_{N_c-1} & \ddots & \vdots & \hat{h}_2 & \hat{h}_1 \\ \hat{h}_1 & \hat{h}_0 & \ddots & \hat{h}_{N_c-2} & \vdots & \hat{h}_2 \\ \hat{h}_2 & \hat{h}_1 & \ddots & \hat{h}_{N_c-1} & \ddots & \vdots \\ \vdots & \hat{h}_2 & \ddots & \hat{h}_0 & \ddots & \hat{h}_{N_c-2} \\ \vdots & \vdots & \ddots & \hat{h}_1 & \ddots & \hat{h}_{N_c-1} \\ \hat{h}_{N_c-2} & \vdots & \ddots & \hat{h}_2 & \ddots & \hat{h}_0 \\ \hat{h}_{N_c-1} & \hat{h}_{N_c-2} & \vdots & \ddots & \hat{h}_1 & \hat{h}_0 \end{bmatrix} \quad (5)$$

Each elements of the equivalent channel matrix is given as

$$\hat{h}_l = \frac{1}{N_c} \sum_{k=0}^{N_c-1} w(k) H(k) \exp\left(j2\pi k \frac{l}{N_c}\right), \quad (6)$$

where $\{H(k); k=0 \sim N_c-1\}$ is the channel gain and $\{w(k); k=0 \sim N_c-1\}$ is the FDE weight. $\hat{\mathbf{n}} = [\hat{n}(0), \dots, \hat{n}(N_c - 1)]^T$ is the noise vector after FDE.

The well-known FDE is based on zero-forcing (ZF) criterion, maximum ratio combining (MRC) criterion, equal-gain combining (EGC) criterion, and minimum mean square error (MMSE) criterion. Their FDE weights are given by [5]

$$w(k) = \begin{cases} 1/H(k), & \text{ZF} \\ H^*(k), & \text{MRC} \\ H^*(k)/|H(k)|, & \text{EGC} \\ H^*(k)/(|H(k)|^2 + (E_s/N_0)^{-1}), & \text{MMSE} \end{cases} \quad (7)$$

Although ZF-FDE can transform the frequency-selective channel into a frequency-nonselctive channel, the noise is enhanced after FDE. On the other hand, however the frequency-diversity gain can be obtained, MRC, EGC, and MMSE-FDE produce the residual ISI after FDE. In these FDE weight, MMSE-FDE can provide the best BER performance [5]. However, the residual ISI remains after MMSE-FDE and this limits the performance improvement.

We introduced THP at the transmitter to suppress the residual ISI after FDE reception and proposed joint THP/FDE in [11]. Since the equivalent channel is represented by a non-causal channel, THP cannot be used directly. We apply QR-

decomposition [17] on the equivalent channel matrix as $\hat{\mathbf{h}} = \mathbf{Q}\mathbf{R}$, where \mathbf{Q} is a unitary matrix and \mathbf{R} is an upper triangular matrix. Since \mathbf{R} is a causal channel, the THP can be applied at the transmitter. With perfect CSI, the residual ISI after FDE reception can be perfectly removed. The joint THP/FDE requires the CSI at both the transmitter and the receiver.

III. JOINT THP/PRE-FDE

Joint THP/pre-FDE that requires no CSI at the receiver is proposed. Figure 1 illustrates the overall system model of joint THP/pre-FDE. Transmitter uses THP and pre-FDE. Pre-FDE uses the same FDE weights as FDE reception, but the pre-FDE weights are normalized to keep the average signal power same as the pre-FDE input signal power [16]. THP structure is illustrated in Fig. 2. THP is a feedback filter having a non-linear modulo operator [7]. The modulo operator is used to prevent the transmit signal amplitude increase. Figure 3 shows the input-output property of the modulo operator. The modulo operator output is expressed as

$$\begin{aligned}\text{Output} &= \{(\text{Re}[\text{Input}] + M) \bmod 2M\} - M \\ &\quad + j\{(\text{Im}[\text{Input}] + M) \bmod 2M\} - jM, \\ &= \text{Input} + 2Mz\end{aligned}\quad (8)$$

where M is the real-valued modulo operation size and z is a complex value (whose real and imaginary parts are an integer) determined so as to satisfy $-M \leq \text{Re}[\text{Output}]$ and $\text{Im}[\text{Output}] < M$.

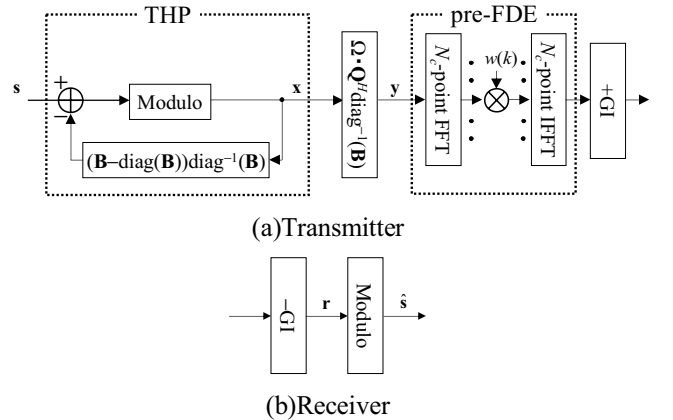


Fig. 1. Transmission system model using joint THP/pre-FDE.

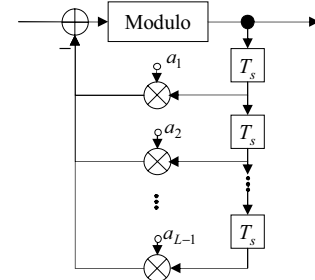


Fig. 2 THP.

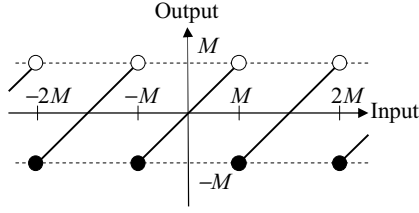


Fig. 3 Input-output property of the modulo operator.

A. LQ-decomposition on the equivalent channel matrix

An equivalent realization of joint THP/FDE based on QR-decomposition is a joint THP/pre-FDE where \mathbf{Q}^H multiplication is done before THP. However, the range of the input to THP is not limited to $[-M, M)$ and hence, the signal constellation may be destroyed by the modulo operator. We apply LQ-decomposition on the equivalent channel matrix as $\hat{\mathbf{h}} = \mathbf{B}\mathbf{Q}$, where \mathbf{B} is a lower triangular matrix and \mathbf{Q} is a unitary matrix. As shown in Fig. 4, \mathbf{Q}^H multiplication can be applied after THP in LQ-decomposition case.

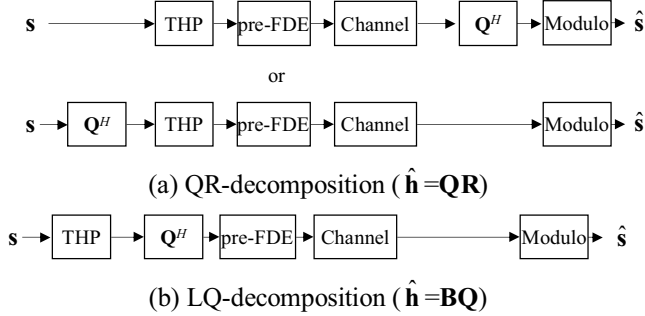


Fig. 4 QR-decomposition and LQ-decomposition.

B. Signal representation

The data modulated symbol block \mathbf{s} is input to THP. THP output vector $\mathbf{x} = [x(0), \dots, x(N_c-1)]^T$ can be expressed as

$$\mathbf{x} = \mathbf{s} - (\mathbf{B} - \text{diag}(\mathbf{B})) \{\text{diag}(\mathbf{B})\}^{-1} \mathbf{x} + 2M\mathbf{z}_t, \quad (9)$$

where $2M\mathbf{z}_t = [2Mz_t(0), \dots, 2Mz_t(N_c-1)]^T$ represents the modulo operation performed in THP and $\text{diag}(\mathbf{A})$ denotes the diagonal matrix obtained by replacing all elements by zero's excluding the diagonal components of \mathbf{A} . The output of THP \mathbf{x} can be rewritten as

$$\mathbf{x} = \text{diag}(\mathbf{B})\mathbf{B}^{-1}(\mathbf{s} + 2M\mathbf{z}_t). \quad (10)$$

After applying THP, \mathbf{x} is multiplied by \mathbf{Q}^H as

$$\mathbf{y} = [y(0), \dots, y(N_c-1)]^T = \Omega \cdot \mathbf{Q}^H \{\text{diag}(\mathbf{B})\}^{-1} \mathbf{x}. \quad (11)$$

Not only \mathbf{Q}^H but also $\{\text{diag}(\mathbf{B})\}^{-1}$ is multiplied to \mathbf{x} to keep the received signal amplitude constant within a block. Ω is the normalization coefficient to keep the average transmit signal power same as that of \mathbf{s} , given by

$$\Omega = \sqrt{\frac{N_c}{\sum_{\tau=0}^{N_c-1} (1/|b_{\tau,\tau}|^2)}}, \quad (12)$$

where $b_{\tau,\tau}$ represents the (τ, τ) th element of \mathbf{B} .

Next, pre-FDE is applied to \mathbf{y} . N_c -point FFT is applied to the signal block \mathbf{y} to transform into the frequency-domain signal. After multiplied by the FDE-weight, the frequency-domain signal is transformed back to the time-domain signal by applying N_c -point IFFT. Then, the N_g -sample GI is inserted and the (N_c+N_g) -signal block is transmitted.

Similar to joint THP/FDE, a concatenation of pre-FDE and the propagation channel is treated as the equivalent channel. Using the equivalent channel matrix $\hat{\mathbf{h}}$ given by Eq. (5), the received signal vector \mathbf{r} can be expressed as

$$\mathbf{r} = \sqrt{\frac{2E_s}{T_s}} C \hat{\mathbf{h}} \mathbf{y} + \mathbf{n}, \quad (13)$$

where $C = \sqrt{N_c / \sum_{k=0}^{N_c-1} |w(k)|^2}$. Eq. (13) can be rewritten, by using Eqs. (10) and (11) and since $\hat{\mathbf{h}} = \mathbf{B}\mathbf{Q}$, as

$$\begin{aligned} \mathbf{r} &= \sqrt{\frac{2E_s}{T_s}} \mathbf{B}\mathbf{Q}\mathbf{C}\mathbf{y} + \mathbf{n} \\ &= \sqrt{\frac{2E_s}{T_s}} \mathbf{B}\mathbf{Q}\Omega\mathbf{C} \cdot \mathbf{Q}^H \{\text{diag}(\mathbf{B})\}^{-1} \mathbf{x} + \mathbf{n}. \quad (14) \\ &= \sqrt{\frac{2E_s}{T_s}} \Omega\mathbf{C} \cdot (\mathbf{s} + 2M\mathbf{z}_t) + \mathbf{n} \end{aligned}$$

It can be seen from Eq. (14) that the ISI can be perfectly removed from the received signal block. Furthermore, the amplitude of the received signal is kept constant in a block. At the receiver, after dividing each elements of the received signal block by $(\sqrt{2E_s/T_s}\Omega\mathbf{C})^{-1}$ (this can be easily estimated at the receiver by transmitting the known pilot), the received signal block is input to the same modulo operator as used in THP. The modulo operator output $\hat{\mathbf{s}} = [\hat{s}(0), \dots, \hat{s}(N_c-1)]^T$ is the decision variable and can be expressed as

$$\begin{aligned} \hat{\mathbf{s}} &= (\sqrt{2E_s/T_s}\Omega\mathbf{C})^{-1} \mathbf{r} + 2M\mathbf{z}_r \\ &= \mathbf{s} + 2M\mathbf{z}_t + 2M\mathbf{z}_r + (\sqrt{2E_s/T_s}\Omega\mathbf{C})^{-1} \mathbf{n}, \quad (15) \end{aligned}$$

where $2M\mathbf{z}_r = [2Mz_r(0), \dots, 2Mz_r(N_c-1)]^T$ represents the modulo operation. If we neglect the perturbation due to AWGN noise, since the real and imaginary parts of the modulo operator output are within $[-M, M)$, then $2M\mathbf{z}_r \approx -2M\mathbf{z}_t$ and we have $\hat{\mathbf{s}} \approx \mathbf{s} + (\sqrt{2E_s/T_s}\Omega\mathbf{C})^{-1} \mathbf{n}$.

C. Received signal-to-noise power ratio after the modulo operator

Assuming $2M\mathbf{z}_r \approx -2M\mathbf{z}_t$ (this holds for very high signal-to-noise power ratio (SNR)), the received SNR after modulo operation can be given by

$$\gamma(t) = \frac{2E_s}{N_0} C^2 \Omega^2 = \frac{2E_s}{N_0} \frac{C^2}{N_c} \left\{ \sum_{\tau=0}^{N_c-1} \frac{1}{|b_{\tau,\tau}|^2} \right\}^{-1}. \quad (16)$$

It can be seen from Eq. (16) that the received SNR after modulo operation depends on the amplitudes of the diagonal elements of the lower triangular matrix \mathbf{B} . In Refs. [10, 11], we pointed out that the amplitudes of the diagonal element of the upper triangular matrix \mathbf{R} drops at symbol positions close to the end of N_c -signal block, thereby degrading the BER performance. In joint THP/FDE, a sequence of N_d ($=N_g$) dummy symbols is inserted in each block to avoid the performance degradation. In joint THP/pre-FDE, since the diagonal components of \mathbf{B} has the similar property of the diagonal components of \mathbf{R} , we also insert a sequence of N_d ($=N_g$) dummy symbols at the end of N_c -data block as illustrated in Fig. 5.

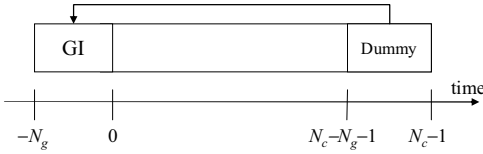


Fig. 5 Block structure.

IV. COMPUTER SIMULATION

The simulation condition is summarized in Table 1. 16QAM and 64QAM data modulation are used. A square-root Nyquist filter [1] with a rolloff factor $\alpha=0.5$ is assumed as the transmit/receive filters. We use EGC-FDE that can provide the best BER performance among four FDE weights presented in Eq. (7) when THP is jointly used. The channel is assumed to be an $L=16$ -path frequency-selective block Rayleigh fading channel having uniform power delay profile. As discussed in Sec. III, we assume the perfect CSI.

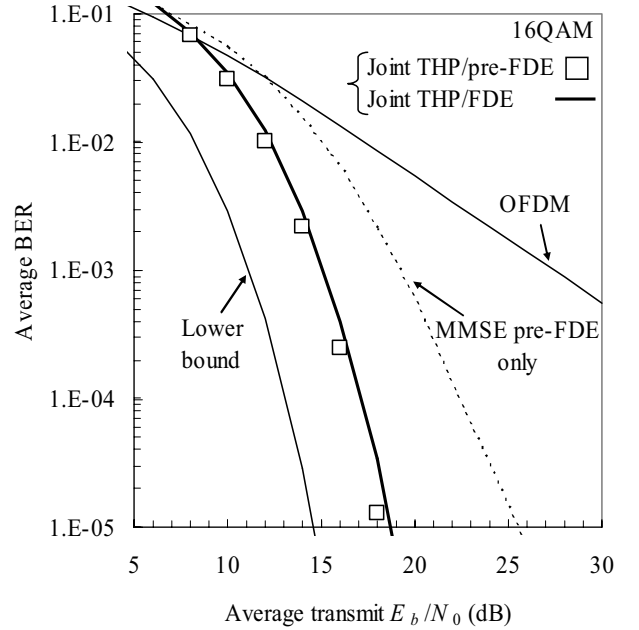
Table 1 Simulation condition

Transmitter	Data modulation	16QAM, 64QAM
	No. of FFT/IFFT points	$N_c=128$
	No. of GI samples	$N_g=16$
	No. of dummy samples	$N_d=N_g$
	FDE	EGC
Channel	Frequency-selective block Rayleigh	
	No. of paths	$L=16$
	Delay time	$\tau=l$
	Power delay profile	Uniform
	CSI	Perfect

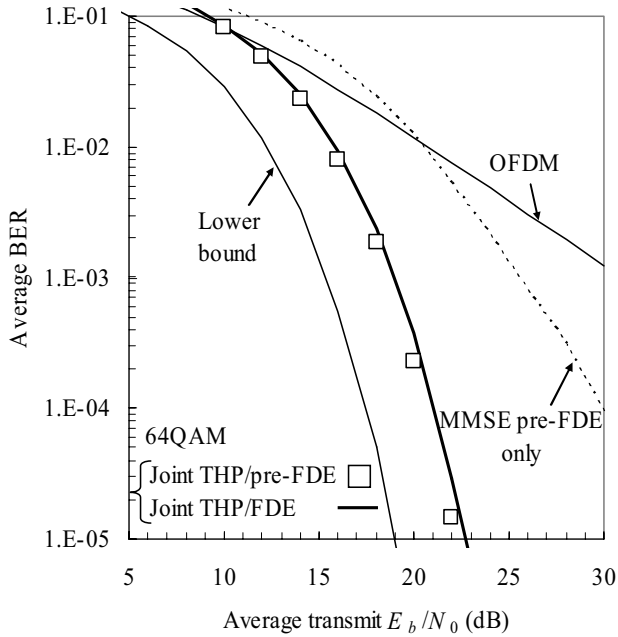
The BER performance of joint THP/pre-FDE is plotted in Fig. 6 as a function of the average transmit bit energy-to-noise power spectrum density $E_b/N_0 = (1/N) \cdot (E_s/N_0) \cdot (N_c + N_g) / (N_c - N_g)$ (where N is the number of bits per symbol). For comparison, the results of joint THP/FDE, MMSE pre-FDE only [16], and orthogonal frequency division multiplexing (OFDM) [18] are also plotted. Because of the frequency-diversity gain, MMSE pre-FDE can provide better BER performance than OFDM. However, due to the residual ISI, the achievable BER performance is degraded

from the theoretical lower-bound [4] and larger performance degradation is seen for 64QAM. On the other hand, joint THP/pre-FDE and joint THP/FDE can remove the residual ISI and hence provide the BER performance closer to the theoretical lower-bound. It should be noted that joint THP/pre-FDE requires the CSI at the transmitter only while joint THP/FDE requires it at both transmitter and receiver. Therefore, the use of joint THP/pre-FDE can simplify the mobile terminal receiver for the downlink.

Fig. 7 plots the probability of the peak-to-average transmit power ratio (PAPR) falling below a certain value. For comparison, the results of OFDM, MMSE pre-FDE, joint THP/FDE, and conventional SC transmission are also plotted. Although OFDM has large PAPR, the conventional SC has a much lower PAPR. Joint THP/FDE only slightly increase the PAPR since the amplitude variation due to THP is suppressed by modulo operation. However, since joint THP/pre-FDE performs pre-FDE after modulo operation, it has the PAPR larger than OFDM. However, at the cost of the PAPR increase, a much better BER performance can be achieved by joint THP/pre-FDE. Joint THP/pre-FDE can be applied to the downlink.



(a) 16QAM



(b) 64QAM

Fig. 6 BER performances.

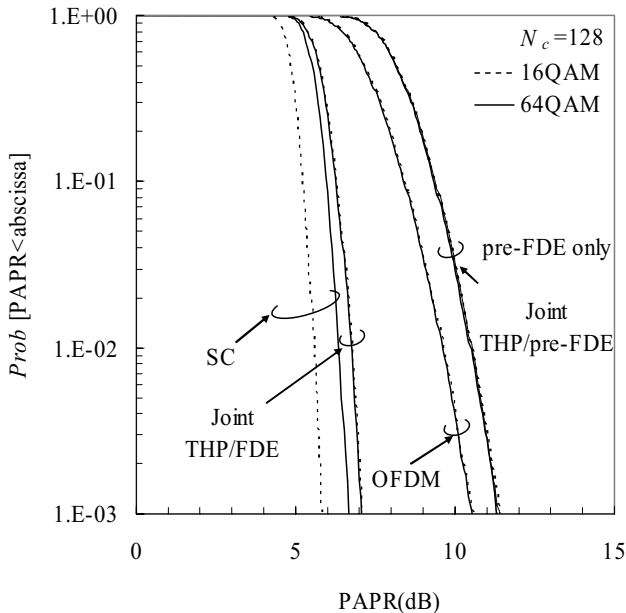


Fig. 7 PAPR distribution.

V. CONCLUSION

In this paper, we presented a joint THP/pre-FDE that requires no CSI at the receiver. We showed by computer simulation that joint THP/pre-FDE significantly improves the downlink BER performance compared to MMSE pre-FDE only and achieves almost the same BER performance as joint THP/FDE at the cost of increased PAPR. Reducing the PAPR is left as an important future study.

REFERENCES

- [1] J. G. Proakis, *Digital communications*, 2nd ed., McGraw-Hill, 1995.
- [2] D. Falconer, S. L. Ariyavisitakul, A. Benyamin-Seeyar, and B. Edison, "Frequency-domain equalization for single-carrier broadband wireless systems," *IEEE Commun. Mag.*, Vol. 40, No. 4, pp. 58-66, Apr. 2002.
- [3] F. Adachi, D. Garg, S. Takaoka, and K. Takeda, "Broadband CDMA techniques," *Special Issue on Modulation, Coding and Signal Processing*, *IEEE Wireless Commun. Mag.*, Vol. 12, No. 2, pp. 8-18, Apr. 2005.
- [4] K. Takeda and F. Adachi, "Bit error rate analysis of DS-SS-CDMA with joint frequency-domain equalization and antenna diversity reception," *IEICE Trans. Commun.*, Vol. E87-B, No. 10, pp. 2991-3002, Oct. 2004.
- [5] T. Itagaki and F. Adachi, "Joint frequency-domain equalization and antenna diversity combining for orthogonal multicarrier DS-SS-CDMA signal transmissions in a frequency-selective fading channel," *IEICE Trans. Commun.*, Vol. E87-B, No. 7, pp. 1954-1963, July 2004.
- [6] M. Tomlinson, "New automatic equalizer employing modulo arithmetic," *Electronics Letters*, Vol. 7, No. 5/6, pp. 138-139, Mar. 1971.
- [7] H. Harashima and H. Miyakawa, "Matched-transmission technique for channels with intersymbol interference," *IEEE Trans. Commun.*, Vol. 20, No. 4, pp. 774-780, Aug. 1972.
- [8] R. H. Fischer, C. Windpassinger, A. Lampe, and J. Huber, "Space-time transmission using Tomlinson-Harashima precoding," *Proc. 4th Intern. ITG conference on source and channel coding*, pp. 139-147, Berlin, Jan. 2002.
- [9] D. Schmidt, M. Johan, F. A. Dietrich, K. Kusume, and W. Utschick, "Complexity reduction for MMSE multiuser spatio-temporal Tomlinson-Harashima precoding," *IEEE International ITG, Duisburg, Germany*, Apr. 2005.
- [10] K. Takeda, H. Tomeba, and F. Adachi, "Single-carrier transmission with joint Tomlinson-Harashima precoding and frequency-domain equalization," *The 3rd IEEE VTS Asia Pacific Wireless Communications Symposium (APWCS)*, pp. 262-266, Daejeon, Korea, Aug. 2006.
- [11] K. Takeda, H. Tomeba, and F. Adachi, "BER performance analysis of joint Tomlinson-Harashima precoding and frequency-domain equalization," *IEEE wireless communications and networking conference (WCNC)*, Hong Kong, Mar. 2007.
- [12] S. Tomasin and N. Benvenuto, "Frequency-domain interference cancellation and nonlinear equalization for CDMA systems," *IEEE Trans. on Wireless Commun.*, Vol. 4, No. 5, pp. 2329-2339, Sep. 2005.
- [13] K. Takeda, K. Ishihara, and F. Adachi, "Downlink DS-SS-CDMA transmission with joint MMSE equalization and ICI cancellation," *Proc. 63rd IEEE Veh. Technol. Conf. (VTC)*, Vol. 4, pp. 1762-1766, May 2006.
- [14] R. Esmailzadeh and M. Nakagawa, "Pre-rake diversity combination for direct sequence spread spectrum mobile communications systems," *IEICE Trans. Commun.*, Vol. E76-B, No. 8, pp. 1008-1015, Aug. 1993.
- [15] I. Cosovic, M. Schnell, and A. Springer, "On the performance of different channel pre-compensation techniques for uplink time division duplex MC-CDMA," *Proc. 58th IEEE VTC*, Vol. 2, pp. 857-861, Oct. 2003.
- [16] F. Adachi, K. Takeda, and H. Tomeba, "Frequency-domain pre-equalization for multicarrier direct sequence spread spectrum signal transmission," *IEICE Trans. Commun.*, Vol. E88-B, No. 7, pp. 3078-3081, July 2005.
- [17] Gene H. Golub, and Charles F. Van Loan, *Matrix computations*, 2nd ed., The Johns Hopkins University Press, 1989.
- [18] S. Hara and R. Prasad, "Overview of multicarrier CDMA," *IEEE Commun. Mag.*, Vol. 35, No. 12, pp. 126-133, Dec. 1997.